High-resolution land seismic imaging via elastic multi-parameter FWI

Camille Martinez, James McLeman*, Mason Phillips, Vlada Avramovic, Tom Rayment, Stuart Schmitt, Mike Varner, Fabio Mancini, DUG Technology; Ahmad Ammar Chahine, Omar Al Mamari

Summary

Conventional workflows to derive imaging results with methods such as reverse-time migration (RTM) impose assumptions on wave propagation, such as the Born approximation, necessitating pre-processed input data that have attenuated parts of the recorded wavefield that do not agree with these assumptions. Such pre-processing can be non-trivial, especially on land data, where stages such as demultiple often require complex modelling and adaptive subtraction workflows. Multi-parameter full-waveform inversion (MP-FWI) imaging offers an alternative approach that harnesses minimally processed field data to generate a high-resolution reflectivity simultaneously with velocity using the full wavefield, eliminating pre-processing steps such as demultiple, and improving illumination in areas of complex geology or surface obstructions. Land seismic data can also often exhibit strong elastic effects that violate the assumptions of acoustic MP-FWI imaging. In this paper, we demonstrate the application of elastic MP-FWI imaging in a desert setting with geological complexity in the near-surface and target depth. We compare the elastic MP-FWI imaging derived reflectivity and velocity with a conventional seismic imaging workflow and the acoustic MP-FWI imaging result.

Introduction

Seismic data processing and imaging methods typically used on land surveys contain a plethora of serial operations, such as denoising, surface-consistent corrections, demultiple, 5D common-offset vector (COV) regularization, and subsurface model building (e.g., Vp, anisotropy, and Q). These pre-processing steps are deployed to modify the recorded wavefield to adhere to the approximations imposed by conventional imaging methods, such as using only primary reflections to build the reflectivity image. Such conventional workflows are non-trivial to execute due to the enormous parameter space that must be traversed to ensure the best possible results, which are time-consuming and contain many subjective judgements. These judgements can be difficult to make on most land seismic data due to the low signal-to-noise ratio. In desert environments, this can be especially true as the primary reflections are often obscured by cultural noise, air waves, surface waves, guided waves, complex multiples generated from various sources, and heterogeneities in the near-surface weathering layer, causing complex distortions of all arrivals passing through it.

An alternative approach makes use of MP-FWI imaging (McLeman et al., 2023). This implementation of FWI decomposes the update kernel into kinematic and dynamic components, enabling the estimation of many subsurface parameters simultaneously (e.g., velocity and reflectivity). The crosstalk between these parameters is further reduced using a novel second-order quasi-Newton optimization scheme (McLeman et al., 2023). The derived velocity model can be used for conventional imaging purposes if required, and the reflectivity generated is suitable for quantitative and structural interpretation. MP-FWI imaging does not rely on the assumptions imposed by conventional imaging algorithms, enabling it to use the full wavefield, including interbed and free-surface multiples. In complex geology, the inclusion of multiples coupled with the least-squares nature of the approach yields improvements in subsurface illumination and amplitude fidelity (Rayment et al., 2023). These applications, however, have traditionally made use of the acoustic approximation which can break down in regions with high impedance contrasts.

In this paper, we consider data acquired in a desert environment and extend the work of Phillips et al. (2024) to demonstrate the successful application of elastic MP-FWI imaging and evaluate how this approach compares to a conventional workflow and acoustic MP-FWI imaging.

Method

The data used in this case study consists of two 3D land seismic surveys acquired in a desert environment. Both surveys were acquired using geophone arrays and vibrator sources in a cross-spread geometry. The surface topology resulted in an acquisition layout that was largely regular, with some irregularities due to surface obstructions. The geology of the region consists of alternating carbonate and clastic sequences, with a steep regional dip with unconformities and faults.

Three workflows were run; the first generated a conventional seismic processing and imaging result. The data were pre-processed with adaptive notch filtering to attenuate the cultural noise, despiking, refraction static corrections, linear and random noise attenuation, surface-consistent deconvolution, demultiple, and 5D COV interpolation. The surface-consistent scaling and residual statics corrections were applied in several passes at various stages. The initial near-surface Vp model was generated using refraction tomography, with the deeper section consisting of smoothed depth-converted stacking velocities. First-break picking was performed using the raw field data, and partially stacked super gathers were used for the velocity analysis. The near-surface Vp model was updated with diving wave FWI, beginning at 5 Hz and stepping up to 12 Hz in five frequency

increments. Minimal data pre-processing was applied to the field data input to diving wave FWI, which included linear noise attenuation and low-frequency incoherent noise attenuation. The deeper section of the Vp model was updated using three passes of RMO tomography. The residual depth errors at several well locations were measured and used to calibrate the anisotropy and Vp models. The pre-processed data was migrated using both COV Kirchhoff pre-stack depth migration (KDM) and RTM.

In parallel to this, acoustic MP-FWI imaging was used to determine updated Vp and reflectivity models. The initial models were derived from the conventional workflow and were smoothed to simulate starting with less mature inputs. This approach was then run in frequency steps up to 30 Hz. The input data to this approach were minimally processed in comparison to the conventional approach. The processing included adaptive notch filtering, despiking, random and linear noise attenuation, and surface consistent corrections. For acoustic MP-FWI imaging, the linear noise attenuation was designed to only remove surface waves and guided shear waves that will not be modelled by the acoustic engine. Note that the reduced pre-processing used does not contain any demultiple or 5D COV regularization, which can be time-consuming to test on land data. The input wavelet for FWI was the theoretical impulse response of the acquisition system. Surface-consistent corrections were applied to the input data to compensate for wavelet distortions caused by the near-surface.

The third workflow partially mimicked the acoustic MP-FWI imaging workflow, but used elastic MP-FWI imaging instead. The initial Vs/Vp model was derived using well information and extrapolated along horizons. Well logs were not available in the near-surface and therefore several initial Vs/Vp models were considered and evaluated.

Results

The updated Vp model generated by acoustic MP-FWI imaging and elastic MP-FWI imaging were evaluated using a Kirchhoff pre-stack depth migration, using the fully pre-processed data as input. Figure 1 compares the COV KDM snail gathers migrated using the initial velocity model, the conventionally-derived velocity model, the acoustic MP-FWI imaging-derived velocity model, and the elastic MP-FWI imaging-derived velocity model. The conventional workflow result shows a reduction in the curvature and "jitter" due to the azimuthal kinematic variations. The acoustic MP-FWI imaging-derived velocity demonstrates kinematic improvements over the conventionally-derived velocity model. The elastic MP-FWI imaging-derived velocity model demonstrates a further improvement in gather flatness, particularly around the high-impedance

contrast at interfaces between the clastic and carbonate sequences.

The structural imaging improvements are shown in Figure 2, with the KDM stack of these results. The conventional workflow significantly improved the mid to long wavelength structure compared to the initial model, resulting in improved bandwidth and structural continuity due to the increase in gather flatness and reduction in jitter on the snail gathers. Additional mid to short wavelength resolution is evident in the acoustic MP-FWI imaging approach, which enables the finer scale structures to be better resolved, as highlighted by the yellow arrows. The elastic MP-FWI imaging result shows a further increase in image focusing and improved in structural simplicity, particularly in and around the carbonate sequences.

The reflectivity generated by acoustic and elastic MP-FWI imaging is demonstrated in Figure 3 and compared with an RTM image from the conventional workflow. Since MP-FWI imaging is a least-squares method that utilizes the full wavefield, the reflectivity derived has a higher fidelity amplitude response and improved illumination. The faults, channels, and unconformities are significantly improved compared with the RTM result, as shown by the yellow arrows. The elastic MP-FWI imaging result demonstrates further improvement, particularly with the increased resolution of the carbonate events. The imaging improvements gained with elastic MP-FWI imaging were achieved directly from the partially pre-processed field data without information supplied by interpretation.

Conclusion

In this paper, we have shown a successful application of elastic MP-FWI imaging on land data from a desert environment. The Vp model derived from elastic MP-FWI imaging demonstrated improved gather flatness, with a reduction in azimuthal kinematic variations and an increase in structural focusing when compared with acoustic MP-FWI imaging and the conventional processing and imaging workflow, particularly around the carbonates. The reflectivity derived from elastic MP-FWI imaging, using minimally pre-processed data, demonstrated a significant uplift compared to the RTM, which used fully pre-processed seismic data.

Acknowledgements

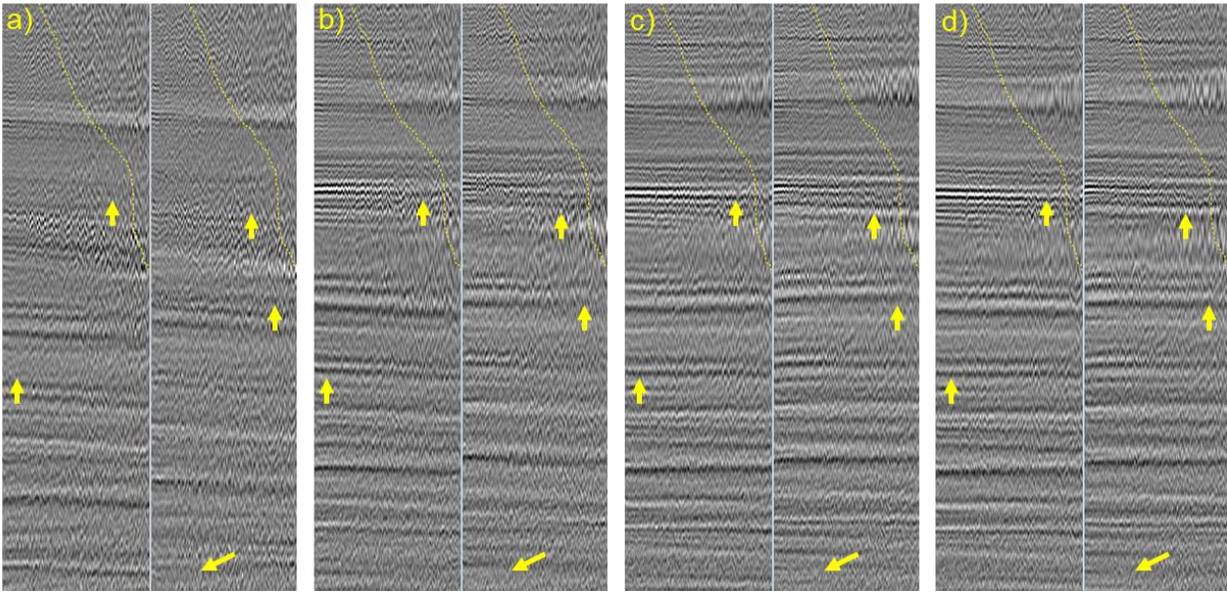# Land seismic elastic multi-parameter FWI imaging

Figure 1: COV KDM snail gathers migrated with the a) initial Vp model, b) conventionally-derived Vp model, c) acoustic MP-FWI imaging-derived Vp model, and d) elastic MP-FWI imaging-derived Vp model for two locations. The yellow dotted line displays a 50-degree angle.
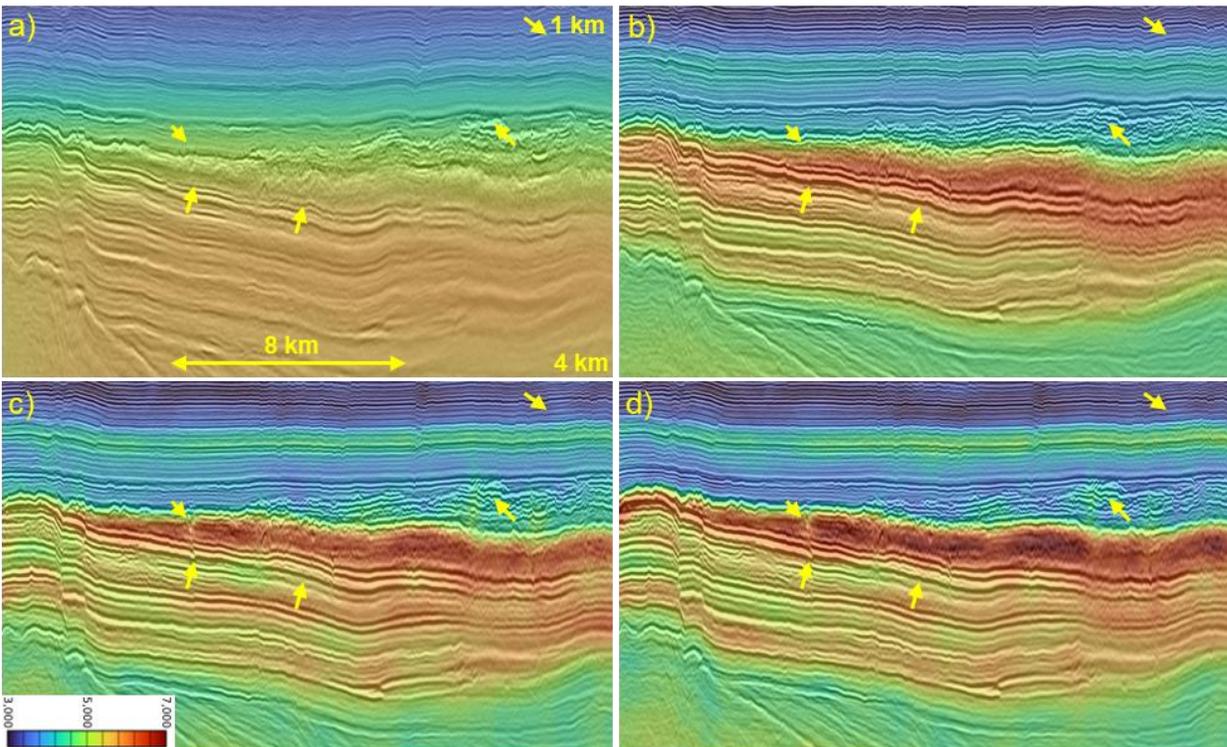

Figure 2: Vp models co-rendered with associated KDM stacks for a) the initial Vp model, b) conventionally-derived Vp model, c) acoustic MP-FWI imaging-derived Vp model, and d) elastic MP-FWI imaging-derived Vp model.

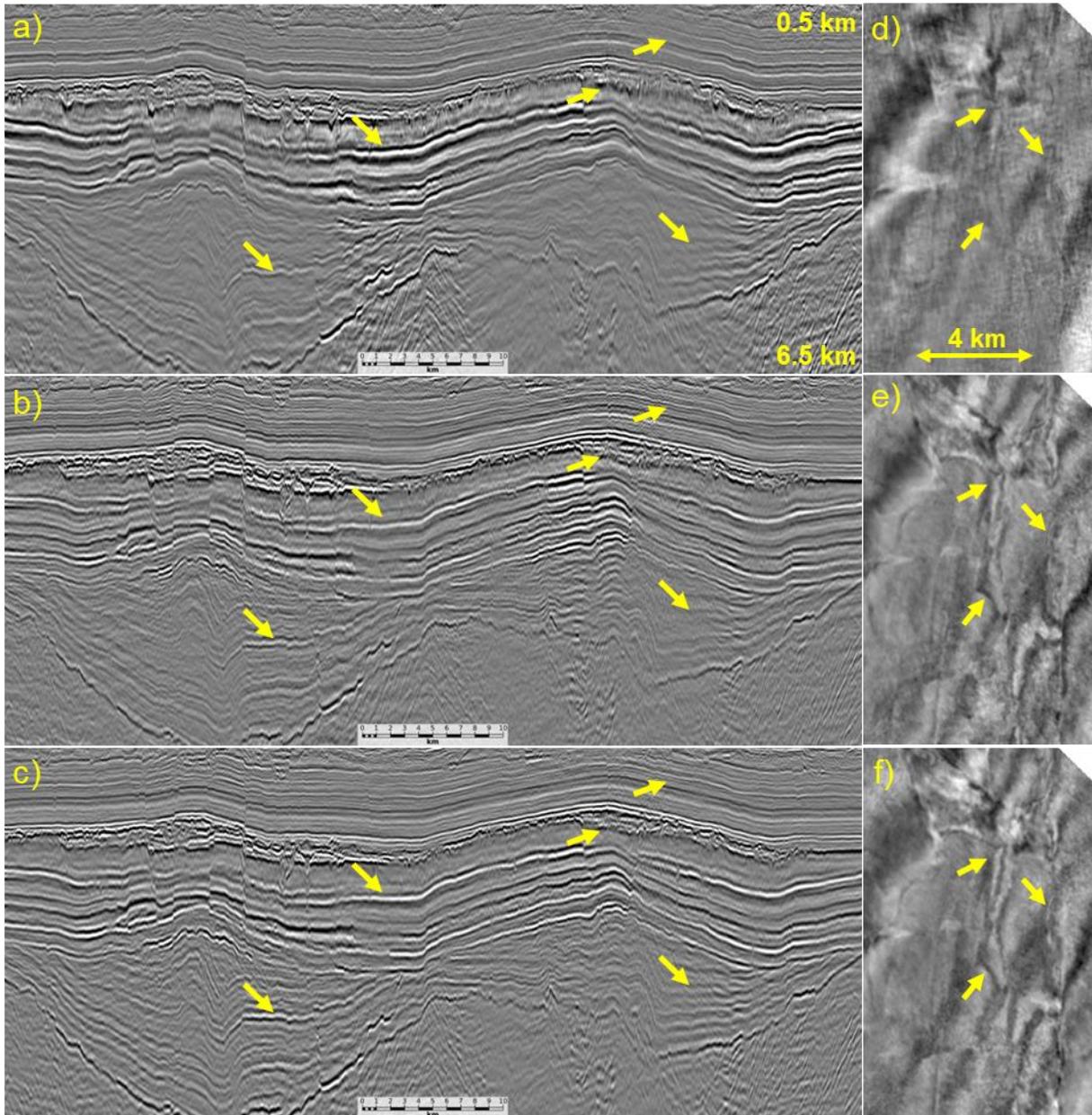# Land seismic elastic multi-parameter FWI imaging

Figure 3: Vertical section through a) 30 Hz RTM of the conventional workflow result using conventionally-derived velocity model, b) the acoustic MP-FWI imaging-derived reflectivity, and c) the elastic MP-FWI imaging-derived reflectivity. Depth slices at 800 m through the corresponding results shown in d), e), and f).